PNAS RESEARCH ARTICLE | MICROBIOLOGY

Live-attenuated virus vaccine defective in RNAi suppression induces rapid protection in neonatal and adult mice lacking mature B and T cells

Gang Chen[a], Qingxia Han[a], Wan-Xiang Li[a], Rong Hai[a,1], and Shou-Wei Ding[a,1]

Edited by Peter Palese, Icahn School of Medicine at Mount Sinai, New York, NY; received December 1, 2023; accepted March 15, 2024

Global control of infectious diseases depends on the continuous development and deployment of diverse vaccination strategies. Currently available live-attenuated and killed virus vaccines typically take a week or longer to activate specific protection by the adaptive immunity. The mosquito-transmitted Nodamura virus (NoV) is attenuated in mice by mutations that prevent expression of the B2 viral suppressor of RNA interference (VSR) and consequently, drastically enhance in vivo production of the virus-targeting small-interfering RNAs. We reported recently that 2 d after immunization with live-attenuated VSR-disabled NoV (NoVΔB2), neonatal mice become fully protected against lethal NoV challenge and develop no detectable infection. Using *Rag1*$^{-/-}$ mice that produce no mature B and T lymphocytes as a model, here we examined the hypothesis that adaptive immunity is dispensable for the RNAi-based protective immunity activated by NoVΔB2 immunization. We show that immunization of both neonatal and adult *Rag1*$^{-/-}$ mice with live but not killed NoVΔB2 induces full protection against NoV challenge at 2 or 14 d postimmunization. Moreover, NoVΔB2-induced protective antiviral immunity is virus-specific and remains effective in adult *Rag1*$^{-/-}$ mice 42 and 90 d after a single-shot immunization. We conclude that immunization with the live-attenuated VSR-disabled RNA virus vaccine activates rapid and long-lasting protective immunity against lethal challenges by a distinct mechanism independent of the adaptive immunity mediated by B and T cells. Future studies are warranted to determine whether additional animal and human viruses attenuated by VSR inactivation induce similar protective immunity in healthy and adaptive immunity-compromised individuals.

virus | vaccine | influenza | RNAi

Significance

Current antiviral vaccines take weeks to elicit protein-based protection via adaptive immunity. Here, we characterized a unique live-attenuated RNA virus vaccine, where attenuation resulted from the elimination of the viral RNAi suppressor and enhanced the production of virus-targeting small-interfering RNAs. We showed that single-dose immunization with the vaccine just 2 d in advance induced full protection in neonatal and adult mutant mice lacking adaptive immunity. Moreover, the immunized mutant mice remained protected against lethal challenge for at least 90 d postvaccination. Human enterovirus-A71, influenza A, and dengue viruses all encode a similar RNAi suppressor, suggesting potential for developing a distinct type of virus vaccine to confer rapid and effective protection in infants and other immune-compromised individuals.

Antiviral RNA interference (RNAi) is a recently recognized mammalian immune response to RNA virus infection (1–14). Within this antiviral immunity, viral double-stranded RNA replicative intermediates (vRI-dsRNA) are processed into 22-nucleotide small interfering RNAs (siRNA) by the Dicer endonuclease (15–17). These virus-derived siRNAs (vsiRNA) are then loaded into RNA-induced silencing complex (RISC) to guide the specific clearance of viral RNA by Argonaute-2 (Ago2). Consistent with its role in antiviral defense, the RNAi pathway is targeted for suppression by diverse mammalian RNA viruses (18). Notably, RNA viruses from the *Flaviviridae*, *Nodaviridae*, *Orthomyxoviridae*, and *Picornaviridae* families encode nonhomologous dsRNA-binding proteins as viral suppressors of RNAi (VSR) to suppress Dicer-dependent production of vsiRNAs during infection (18). Prior to the demonstration of antiviral RNAi in mammals, it is well established that the conserved long dsRNA→siRNA pathway of RNAi directs an essential defense mechanism against viruses in invertebrates and plants (19, 20).

Much is known about the induction and suppression of antiviral RNAi in mice by Nodamura virus (NoV), a member of the *Nodaviridae* that causes lethal infection in suckling mice and hamsters (10, 21). The bipartite positive-strand RNA genome of the mosquito-transmitted NoV encodes three functional proteins, A, B2, and capsid protein. Protein A (RNA-dependent RNA polymerase, RdRP) and capsid protein are translated from genomic RNAs 1 and 2, respectively. The B2 protein is expressed from RNA 3, a subgenomic RNA of RNA 1 synthesized after RNA 1 replication (22). B2 is the VSR and the genus-conserved arginine at position 59 (R59) of B2 is essential for binding to dsRNA and for suppressing Dicer processing of long dsRNA into siRNAs (23). Unlike wild-type NoV, infection with NoV mutants expressing either no B2 (NoVΔB2) or B2^{R59Q} (NoVmB2) induces no signs of disease in suckling mice and both attenuated NoV mutants are cleared within a week of intraperitoneal (IP) injection upon reaching the peak of accumulation at 3 d postinoculation (2, 10). In adult *Rag1*$^{-/-}$ mice, which produce no mature B and T cells, NoV also causes lethal disease and both NoVΔB2

Competing interest statement: S.-W.D. declares to be named as an inventor on an issued patent (US 10,034,929B2), claiming subject matter related to the use of an attenuated virus defective in RNAi suppression as a vaccine to induce antiviral protection described in this paper. The other authors declare that they have no conflict of interest.

This article is a PNAS Direct Submission.

[1]To whom correspondence may be addressed. Email: ronghai@ucr.edu or shou-wei.ding@ucr.edu.

This article contains supporting information online at https://www.pnas.org/lookup/suppl/doi:10.1073/pnas.2321170121/-/DCSupplemental.

Published April 17, 2024.

and NoVmB2 are as attenuated as in wild-type suckling mice. NoV RNA replication is potently inhibited by the RNAi pathway requiring both Dicer and the slicer activity of Ago2. In the absence of the VSR activity to suppress vsiRNA biogenesis, both of the attenuated NoV mutants trigger production of abundant NoV vsiRNAs by Dicer in the infected mouse embryonic fibroblasts and suckling and adult mice. These vsiRNAs accumulate in RNAi-active RISC capable of directing Ago2-mediated, vsiRNA-guided RNA cleavage. Moreover, the vsiRNAs made in vivo by mouse immune system in response to NoVΔB2 infection circulated systemically in the bloodstream, remained readily detectable in the mice long after NoVΔB2 clearance, and mediated RNA sequence homology-dependent inhibition of secondary infection by the unrelated Sindbis virus engineered to be targeted by these vsiRNAs (13, 14). Notably, immunization of neonatal BALB/c mice with live-attenuated VSR-disabled NoVΔB2 induced full protection against lethal NoV challenge at 2 d postimmunization (14), which is approximately a week earlier compared to the live-attenuated virus vaccines that activate the adaptive immunity (24).

In this work, we examined the hypothesis that the adaptive immunity mediated by B and T lymphocytes is dispensable for the protective antiviral immunity triggered by immunization with NoVΔB2. Our results demonstrate that the live-attenuated NoVΔB2, known to trigger the production of highly abundant virus-targeting vsiRNAs in vivo, induced rapid protection in both neonatal and adult mutant mice lacking mature B and T lymphocytes. Moreover, the induced protection remained effective in the immunized mutant mice for at least 90 d after a single-shot injection.

Results

Full Protection of Neonatal *Rag1*$^{-/-}$ Mice Lacking Mature B and T Cells Induced by Immunization with a Mutant RNA Virus Attenuated by Inactivating the Viral RNAi Suppressor Activity. Our previous studies revealed rapid activation of full protection of neonatal BALB/c mice from lethal dose of wild-type NoV infection at 2 d postimmunization with live NoVΔB2, a NoV mutant attenuated by the loss of B2-VSR expression (14). To determine the dispensability of the adaptive immune system, we performed NoVΔB2 immunization in *Rag1*$^{-/-}$ mice lacking mature B and T lymphocytes (25) due to the knockout of recombination activating gene 1 (RAG1). In brief, we first immunized neonatal *Rag1*$^{-/-}$ mice through IP injection with live or UV-killed NoVΔB2, and 2 d later, challenged the immunized mice with a lethal dose of NoV. The outcomes reveal that all of the neonatal mice immunized with killed NoVΔB2 developed hind limb paralysis and succumbed within 2 wk postchallenge with NoV (Fig. 1*A*). By contrast, none of the 10 neonatal mice immunized with live NoVΔB2 exhibited any signs of disease up to 4 wk after NoV challenge (Fig. 1*A*). As described previously for BALB/c neonatal mice (14), therefore, immunization with live NoVΔB2 for only 2 d in advance induced rapid and complete protection of neonatal *Rag1*$^{-/-}$ mice against lethal NoV challenge.

Similarly, the suckling *Rag1*$^{-/-}$ mice immunized with live NoVΔB2, but not with killed NoVΔB2, were fully protected when they were challenged with NoV at 14 d postimmunization (Fig. 1*B*). Our previous results showed that NoV was undetectable by either Western blotting or RT-qPCR in the NoVΔB2-immunized neonatal

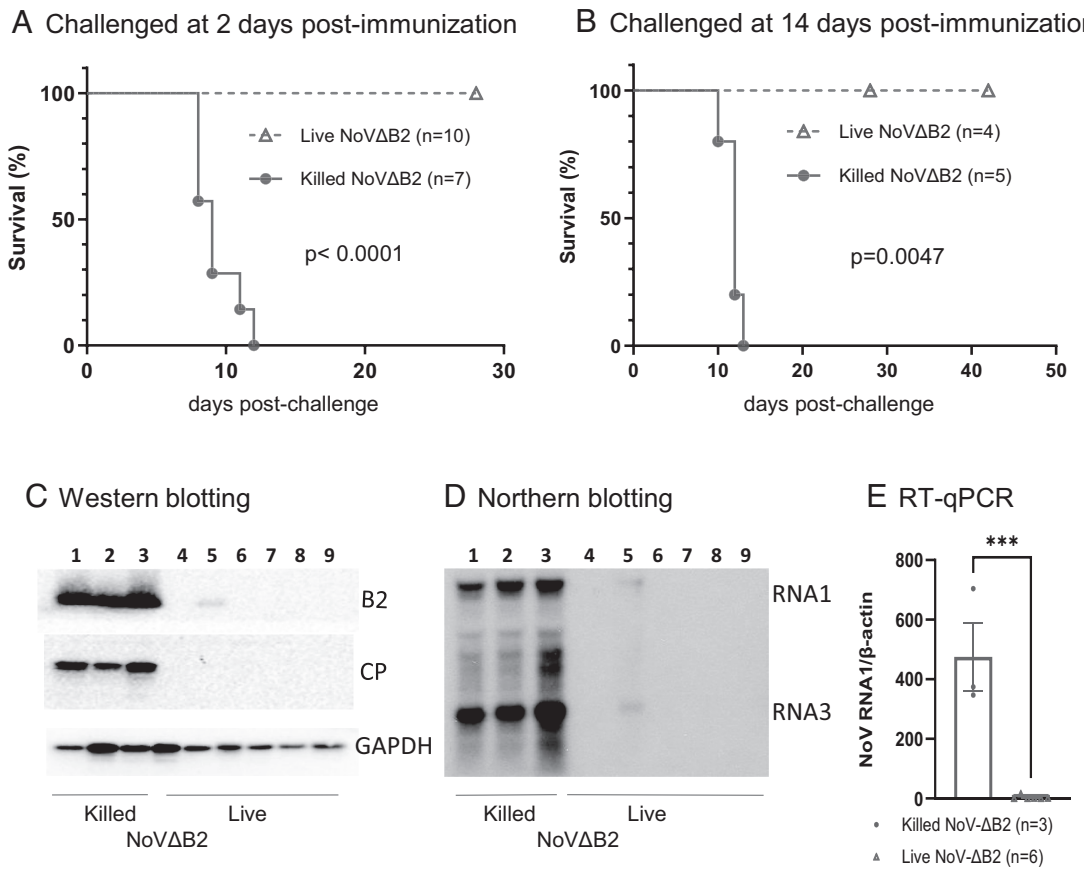

Fig. 1. Rapid induction of protection by the live-attenuated NoVΔB2 in neonatal *Rag1*$^{-/-}$ mice. (*A* and *B*) Newborn *Rag1*$^{-/-}$ mice were immunized with live or killed NoVΔB2 and 2 (*A*) or 14 (*B*) d later, challenged with a lethal dose of NoV. Survival curves were compared using a log rank (Mantel-Cox) test. (*C*–*E*) Viral load was determined by Western blotting (*C*), Northern blotting (*D*), and RT-qPCR (*E*) at 5 d postchallenge in each mouse that was immunized for 14 d as those in panel *B*.

BALB/c mice after challenge infection at 2 d postimmunization (14). Here, we examined whether NoV established infection in the immunized *Rag1*$^{-/-}$ mice after challenge infection at 14 d postimmunization. It is known that NoV replicates to the highest levels in the hind limb muscle tissues at 4 d postinoculation by IP injection (2, 10). At 5 d after challenge inoculation with NoV, we detected accumulation of abundant viral B2 and capsid proteins, as along with viral genomic and subgenomic RNAs, by Western and Northern blotting assays and/or RT-qPCR in the suckling *Rag1*$^{-/-}$ mice immunized with killed NoVΔB2 (Fig. 1 *C*–*E*), which is consistent with the development of lethal disease in these mice (Fig. 1*B*). In contrast, these viral RNAs and proteins were all undetectable in five of the six examined suckling mice immunized with live NoVΔB2 (Fig. 1 *C*–*E*). NoV infection was successful in one of these mice immunized with live NoVΔB2 although the viral capsid protein was undetectable and the viral B2 protein and genomic/subgenomic RNAs accumulated only to low levels in this mouse (Fig. 1 *C*–*E*). Therefore, the induced immunity remained protective against NoV infection in the suckling *Rag1*$^{-/-}$ mice at 14 d postimmunization with live NoVΔB2. Together, our results show that immunization of neonatal *Rag1*$^{-/-}$ mice with live NoVΔB2 induced full protection against lethal NoV challenge at both 2 and 14 d postimmunization, indicating induction of a distinct type of protective antiviral immunity independent of the adaptive immune system in neonatal mice.

Rapid and Full Protection of Adult *Rag1*$^{-/-}$ Mice Induced by Immunization with Live NoVΔB2. Adult BALB/c and C57BL/6 mice are resistant to NoV and develop no signs of disease after NoV inoculation (10, 21). However, adult *Rag1*$^{-/-}$ mice are as susceptible as wild-type neonatal mice to NoV infection and the virulence and abundant accumulation of NoV in both types of mice require the expression of a functional VSR-B2, which does not appear to alter the induction levels of interferon-stimulated genes or the activation of global RNA cleavages by RNase L (10). To determine whether NoVΔB2 also is an active immunogen in adult mice, 6- to 8-wk-old *Rag1*$^{-/-}$ mice were immunized with live NoVΔB2 using killed NoVΔB2 and buffer as controls. At 2 or 14 d postimmunization, the three groups of adult *Rag1*$^{-/-}$ mice were all challenged with a lethal dose of NoV.

We found that all of the adult *Rag1*$^{-/-}$ mice immunized for either 2 or 14 d with live NoVΔB2 in independent experiments survived the challenge infection without any signs of disease up to 6 wk (Fig. 2 *A* and *B*). In contrast, both groups of control mice exhibited significant weight loss and almost all died before 18 d postchallenge (Fig. 2 *A* and *B*). These results show that immunization with live NoVΔB2 induced rapid and complete protection of adult *Rag1*$^{-/-}$ mice against lethal NoV challenge and that the induced immunity remained protective at 2 wk postimmunization.

Previous studies indicated that microbiota do not play an important role in regulating antibody responses to vaccines in adult mice (26, 27). We found that immunization with live but not killed NoVΔB2 also induced highly effective protection in adult *Rag1*$^{-/-}$ mice depleted of the intestinal microbiota by antibiotics treatment (*SI Appendix*, Fig. S1 *A*–*C*). Moreover, *Rag2*$^{-/-}$ $\gamma c^{-/-}$ double knockout mice lack B and T lymphocytes as well as natural killer cells (28, 29). We found that adult *Rag2*$^{-/-}$ $\gamma c^{-/-}$ mice immunized with live but not killed NoVΔB2, were also fully protected when they were challenged with NoV at 14 d postimmunization (*SI Appendix*, Fig. S2). Together, our results show that immunization of adult *Rag1 or Rag2* knockout mice with live NoVΔB2 induced full protection against lethal NoV challenge at both 2 and 14 d postimmunization, indicating induction of a protective antiviral immunity independent of the adaptive immune system in adult mice.

Immunization with Live NoVΔB2 Induces Long-Lasting Protection in Adult *Rag1*$^{-/-}$ Mice. Vaccine efficacy studies in adult mice routinely assay for protection by B and T lymphocytes after immunization for 6 wk or longer. For a comparison, we also determined whether the distinct protective immunity induced by live NoVΔB2 in adult *Rag1*$^{-/-}$ mice remained active at 42 d postimmunization when NoVΔB2 accumulation was undetectable (*SI Appendix*, Fig. S3). In the adult *Rag1*$^{-/-}$ mice immunized with killed NoVΔB2, NoV

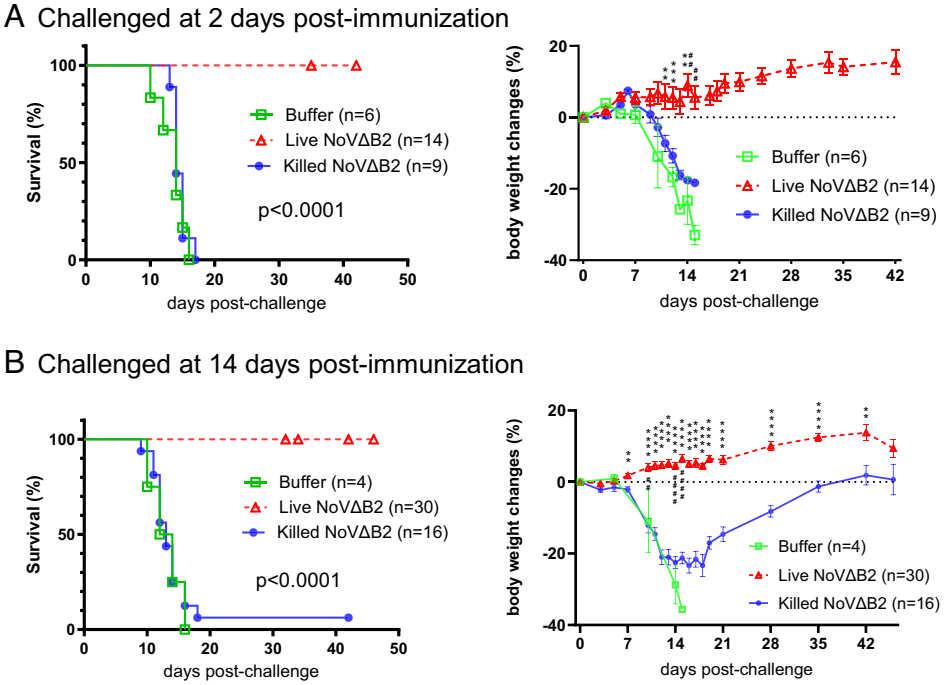

Fig. 2. Rapid induction of protection by the live-attenuated NoVΔB2 in adult *Rag1*$^{-/-}$ mice. (*A* and *B*) Survival and body weight change of the adult *Rag1*$^{-/-}$ mice that were immunized with buffer, live or killed NoVΔB2 and 2 (*A*) or 14 (*B*) d later, challenged with a lethal dose of NoV. Survival curves were compared using a log rank (Mantel-Cox) test whereas body weight changes between immunization by live and killed NoVΔB2 were analyzed by Multiple unpaired *t* tests.

infection caused significant weight loss and all the challenged mice died in contrast to those immunized but not challenged (Fig. 3*A*). However, all the adult *Rag1*$^{-/-}$ mice immunized with live NoVΔB2 survived NoV inoculation without significant weight loss (Fig. 2*C*). Moreover, we observed similarly efficient protection against lethal challenge in adult *Rag1*$^{-/-}$ mice when a 100-fold lower concentration of live NoVΔB2 was used for immunization (Fig. 3*A*). These findings show that the induced antiviral immunity remained fully protective at 6 wk postimmunization with live-attenuated NoVΔB2 in a single injection in adult *Rag1*$^{-/-}$ mice defective in the classical adaptive immunity.

We further investigated the durability of the protective antiviral immunity induced in the adult *Rag1*$^{-/-}$ mice by immunization with the NoV mutant attenuated by abolishing the VSR activity. In the first set of experiments, we performed NoV challenge infection of the immunized adult *Rag1*$^{-/-}$ mice at 90 d postimmunization with live or killed NoVΔB2 in a single injection (Fig. 3*B*). All of the mice immunized with killed NoVΔB2 for 90 d suffered significant weight loss and died before 20 d after NoV inoculation. However, only one of the 12 *Rag1*$^{-/-}$ mice immunized with live NoVΔB2 for 90 d did not survive NoV inoculation, whereas all of the remaining immunized *Rag1*$^{-/-}$ mice were healthy and exhibited no obvious weight loss under the pathogen-free conditions (Fig. 3*B*). These results revealed that the protective antiviral immunity established in the adult *Rag1*$^{-/-}$ mice by immunization with live NoVΔB2 remains effective 3 mo after immunization, indicating induction of a long-lasting protective antiviral immunity in adult mice in the absence of the classical adaptive immunity.

In the second set of experiments, we determined whether parental immunization in the adult *Rag1*$^{-/-}$ with live NoVΔB2 triggers

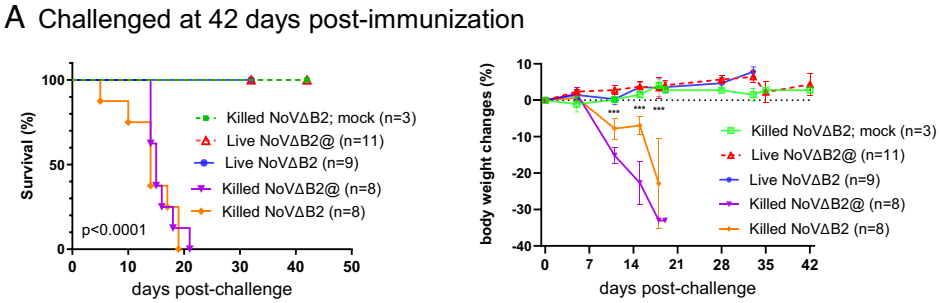

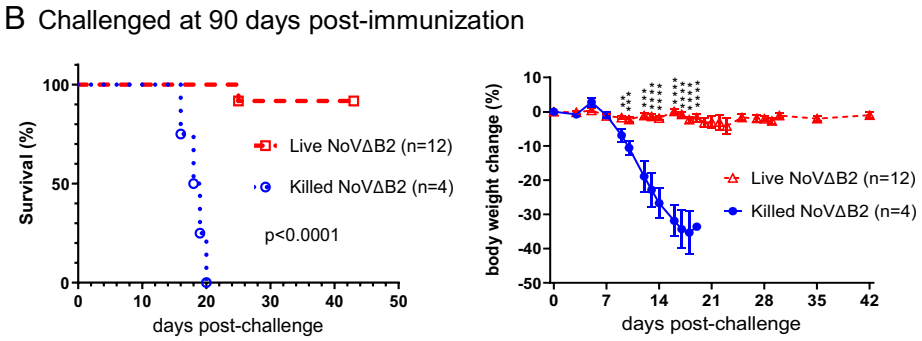

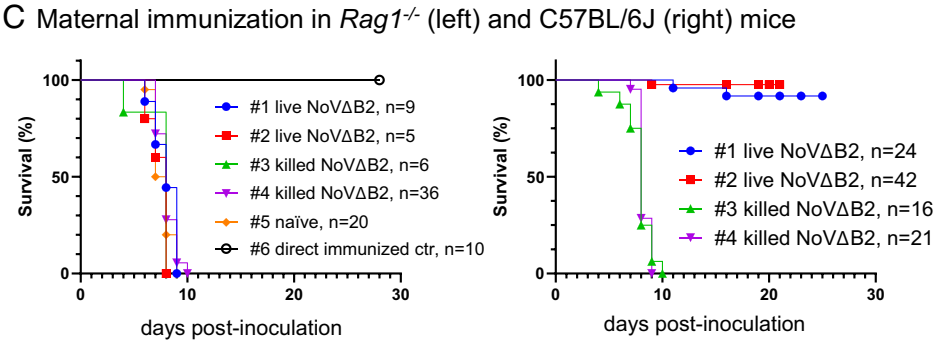

	#1	#2	#3	#4	#5	#6
Mother	Live NoVΔB2	Live NoVΔB2	killed NoVΔB2	killed NoVΔB2	naive	naive
Father	killed NoVΔB2	Live NoVΔB2	Live NoVΔB2	killed NoVΔB2	killed NoVΔB2	naive

Fig. 3. Induction of long-lasting protection by the live-attenuated NoVΔB2 in adult *Rag1*$^{-/-}$ mice. (*A* and *B*) Survival and body weight change of the adult *Rag1*$^{-/-}$ mice that were immunized with live or killed NoVΔB2 and 42 (*A*) or 90 (*B*) d later, challenged with a lethal dose of NoV. When not challenged (mock), all adult mice immunized with killed NoVΔB2 remained healthy (*A*). @ indicated the use of a 100-fold lower concentration of live or killed NoVΔB2 for immunization. (*C*) Survival of the neonatal mice born from *Rag1*$^{-/-}$ (*Left*) or C57BL/6 J (*Right*) parents immunized with live or killed NoVΔB2 (as indicated at the bottom) after challenge at 6 to 8 d after birth with a lethal dose of NoV. Protection against NoV infection was observed only for the neonatal mice born from C57BL/6 J mothers immunized with live NoVΔB2. Unless directly immunized with live NoVΔB2 (#6), all neonatal mice of unimmunized *Rag1*$^{-/-}$ parents (naïve) succumbed to NoV infection as expected.

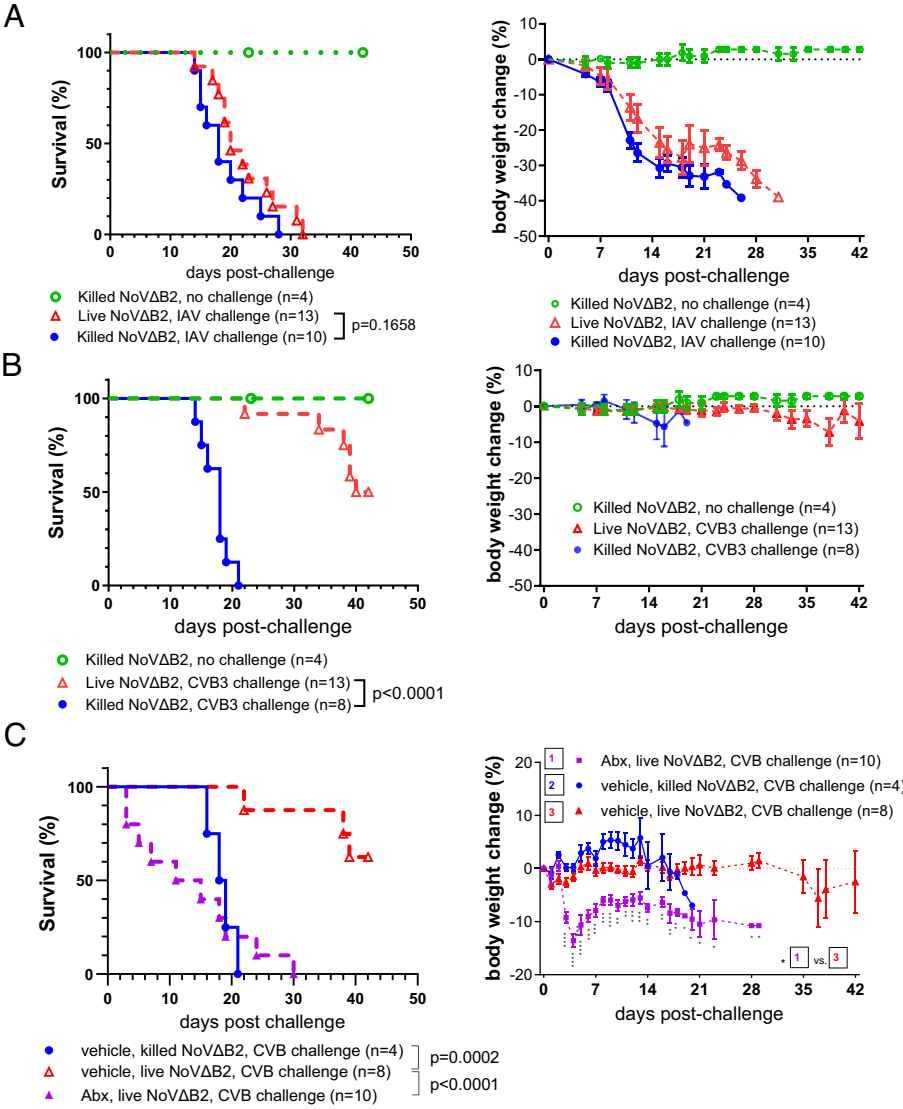

Fig. 4. Virus-specific protection of adult *Rag1*$^{-/-}$ mice induced by immunization with NoVΔB2. (*A* and *B*) Survival and body weight change of adult *Rag1*$^{-/-}$ mice that were immunized with live or killed NoVΔB2 and 42 d later, challenged with a lethal dose of IAV/PR8 (*A*) or CVB3 (*B*). (*C*) Survival and body weight change of the adult *Rag1*$^{-/-}$ mice with or without microbiome depletion that were immunized with live or killed NoVΔB2 and 42 d later, challenged with a lethal dose of CVB3. The intestinal microbiome was depleted by adding an oral antibiotics cocktail (Abx) or vehicle to drinking water for 3 d before immunization and throughout the course of the experiment. Statistical differences in survival (*Left*) and body weight changes (*Right*) are shown respectively by *P* value and the number of the star symbol between immunization with live NoVΔB2 in vehicle- and Abx-treated mice (*$P < 0.05$; **$P < 0.01$; ***$P < 0.001$; ****$P < 0.0001$).

protective antiviral immunity in the offspring. To this end, adult female and male *Rag1*$^{-/-}$ mice were immunized with live or killed NoVΔB2 and 4 wk later, they were used as breeders in various different combinations (Fig. 3*C*). We found that the neonatal mice born from all of these *Rag1*$^{-/-}$ parents were highly susceptible to NoV challenge and succumbed within 10 d postinfection with NoV (Fig. 3*C*). In contrast, maternal immunization in the adult C57BL/6 mice with live but not killed NoVΔB2 triggered protective antiviral immunity in the offspring against lethal NoV challenges (Fig. 3*D*), consistent with previous findings (21). These findings indicate that while immunization with live NoVΔB2 triggers long-lasting protective antiviral immunity in the absence of adaptive immunity, the induced protection does not appear to pass onto the offspring of the immunized *Rag1*$^{-/-}$ mice.

Virus-Specific Protective Immunity Induced in Adult *Rag1*$^{-/-}$ Mice by Live NoVΔB2. We next investigated whether the protective antiviral immunity induced in *Rag1*$^{-/-}$ mice by immunization with live NoVΔB2 is virus-specific. At 42 d postimmunization with live or killed NoVΔB2, the immunized adult *Rag1*$^{-/-}$ mice were challenged with a lethal dose of Influenza A virus (IAV-PR8) or Coxsackievirus B3 (CVB3). IAV-PR8 is a negative-strand RNA virus in the *Orthomyxoviridae* and both *Rag1*$^{-/-}$ and *Rag2*$^{-/-}$ mice develop a lethal infection after intranasal inoculation (30, 31). We found that *Rag1*$^{-/-}$ mice immunized with either live or killed NoVΔB2 showed continuous weight loss after IAV-PR8 challenge and all succumbed to infection (Fig. 4*A*). These results indicate that the antiviral immunity induced in *Rag1*$^{-/-}$ mice by immunization with live NoVΔB2 did not confer protection to IAV-PR8.

CVB3 is a positive-strand RNA virus in the *Picornaviridae* and all *Rag1*$^{-/-}$ mice die after CVB3 infection via IP injection (32). We found that *Rag1*$^{-/-}$ mice immunized with killed NoVΔB2 remained highly susceptible to CVB3 (Fig. 4*B*). Interestingly, we observed partial protection of the *Rag1*$^{-/-}$ mice immunized with live NoVΔB2 against CVB3 challenge (Fig. 4*B*). Nevertheless, we detected no protection against CVB3 infection in the live NoVΔB2-immunized adult *Rag1*$^{-/-}$ mice depleted of the intestinal microbiota (Fig. 4*C*), in contrast to the protection against lethal challenge by NoV (*SI Appendix*, Fig. S1*C*). These findings indicate that the protective antiviral immunity induced in *Rag1*$^{-/-}$ mice by immunization with live NoVΔB2 is virus-specific and ineffective against heterologous RNA viruses.

Discussion

In this work, we examined the protective antiviral immunity induced in mice by immunization with a live-attenuated VSR-disabled RNA virus vaccine, NoVΔB2. The RNA-based virus-specific antiviral

responses elicited by NoVΔB2 have been extensively characterized in previous studies (2, 3, 10, 13, 14). In response to the immunization with NoVΔB2 by IP injection, mice produce highly abundant NoV-specific vsiRNAs that are readily detectable in limb skeletal muscle tissues by Northern blotting (2, 10, 13, 14). These vsiRNAs also enter the bloodstream for systemic circulation and remain detectable in the immunized mice at least 20 d after NoVΔB2 is cleared (14). Notably, these vsiRNAs produced by the mouse immune system accumulate in the RISC complex exhibiting the activity to direct specific target RNA slicing by Ago2 (10), providing direct evidence for their role as the specificity-determinants of the induced antiviral immunity. NoVΔB2-immunized mice also specifically suppress the accumulation of a recombinant Sindbis virus carrying a NoV RNA sequence and this vsiRNA-mediated suppression of the challenge infection becomes more effective in the type I interferon (IFN) receptor knockout mice (13). Moreover, LGP2 (laboratory of genetics and physiology 2), a known IFN-stimulated gene (ISG) product, inhibits Dicer processing of both artificial and viral dsRNA (12, 13, 33), which further indicates RNAi suppression by IFN signaling. However, compared to *Rag1*$^{-/-}$ mice, neither the production of NoV-specific vsiRNAs nor the assembly of the slicing-competent vsiRNAs-RISC is enhanced in *STAT1*$^{-/-}$ *STAT2*$^{-/-}$ mice completely defective in IFN signaling although NoVΔB2 is cleared in both mutant mice (10). Thus, a better understanding of the interplay between the IFN- and RNAi-dependent antiviral responses requires further mechanistic studies using in vivo models (17, 34).

Our findings from this work show that the protective antiviral immunity induced by a single shot with live NoVΔB2 is both virus-specific and long-lasting, which are the same as those virus vaccines that activate the adaptive immunity. However, the protective immunity induced by immunization with NoVΔB2 exhibits several distinct features compared to the currently available virus vaccines.

Ensuring global protection against infectious diseases demands the consistent innovation and use of diverse vaccination strategies (24, 35–37). However, only a few approved vaccines (e.g., poliovirus and hepatitis B virus) are currently available for the protection of infants younger than 12 mo (24, 35, 38, 39). Our studies showed that after immunization with live NoVΔB2, neonatal BALB/c and *Rag1*$^{-/-}$ mice became fully protected against lethal NoV challenge and exhibited no signs of disease (14) (Fig. 1). Moreover, NoV accumulation was undetectable in most or all of the immunized BALB/c and *Rag1*$^{-/-}$mice following NoV inoculation, indicating efficient inhibition of the challenge infection in newborn mice due to the induced antiviral responses. Our results further demonstrated that the adaptive immunity mediated by B and T lymphocytes, which is essential for protection by currently available virus vaccines, is dispensable for the protective immunity activated by immunization with the live-attenuated VSR-disabled NoVΔB2. Full protection was established 2 d after immunization in both neonatal and adult *Rag1*$^{-/-}$ mice against lethal challenge and the immunized *Rag1*$^{-/-}$ mice remained fully protected against challenge inoculation at least 3 mo after the single-shot immunization. These distinct features of NoVΔB2-induced protection align with the earlier conclusion that enhanced production of the circulating and stably maintained virus-targeting vsiRNAs confers antiviral protection by the RNAi pathway in mice immunized with the live-attenuated VSR-disabled virus vaccine (10, 13, 14).

Several human RNA viruses including human enterovirus-A71, flaviviruses, and influenza viruses (4, 5, 7, 40), encode dsRNA-binding VSRs and trigger significantly enhanced vsiRNA production and infection defects in human cells when their VSR is rendered nonfunctional (18). Thus, there is potential to develop similar live-attenuated VSR-disabled virus vaccines against these viruses (41–43), especially for the protection of infants and individuals with dysfunctional adaptive immunity. Presumably, VSRs encoded by additional human viruses may be identified by available approaches (18) to facilitate the development of similar live-attenuated VSR-disabled virus vaccines. Compared to a few epitopes recognized by adaptive immunity, almost all regions of the viral RNAs are targeted for antiviral RNAi by a large pool of overlapping vsiRNAs produced during the immune response to VSR-disabled virus infection (15–18, 23, 44). Consequently, it will be of interest to determine whether VSR-disabled live-attenuated virus vaccines confer a broad spectrum of protection against diverse virus strains.

Materials and Methods

Mice. C57BL/6 J, *Rag1*$^{-/-}$ (B6.129S7-*Rag1*^{tm1Mom}/J) and *Rag2*$^{-/-}$ γc$^{-/-}$ (C;129S4-*Rag2*$^{tm1.1Flv}$ *Il2rg*$^{tm1.1Flv}$/J) mice (Strain #:000664, 002216, and 014593, respectively) were purchased from the Jackson Laboratory (Sacramento, California). Animals were housed and bred in the Animal Resources Facility under specific pathogen-free conditions according to the guidelines described under the federal Animal Welfare Regulations Act. All animal procedures were approved by the Institutional Animal Care and Use Committee at the University of California, Riverside.

Viruses. Nodamura virus (NoV) and its mutant NoVΔB2 were described previously (2). NoVΔB2 contains three-point mutations in RNA1 to block B2 translation; however, the genetic change in the mutant virus doesn't alter the amino acid sequence of the viral replicase encoded by RNA1 or the B1 protein, which is identical in sequence to the C-terminal region of the viral replicase and is translated from RNA3 without a known function. All virus stocks were prepared and titrated as described previously (2, 10) and diluted in 1× Dulbecco's modified Eagle's medium (DMEM, Gibco) supplemented with 0.3% BSA (Invitrogen) in fresh for mice injection.

The mouse-adapted CVB3 H3 strain virus stock kindly provided by Dr. Jeff Bergelson, was prepared as described in literature (45, 46) with minor modifications. Briefly, viral RNA genomes were prepared via in vitro RNA transcription from pH3 plasmid and transfected into 293 T cells. The cell culture supernatant containing viral particles was then collected on day-3 posttransfection. After further amplification in 293 T cells, CVB3 particles were purified using ultraspeed centrifugation and resuspended in PBS complemented with 0.1% BSA. Virus stock was frozen in aliquot at −80 °C after being titrated using the TCID50 method in 293 T cells cultured in a 96-well plate. This same virus stock was used in all the CVB3 inoculation experiment in mice after proper dilution in PBS plus 0.1% BSA.

Influenza A virus was cultured in embryonated chicken eggs. Influenza A Puerto Rico/8/34(H1N1) virus (IAV/PR8) was amplified in 10-d-old specific pathogen-free (SPF) chicken embryonated eggs (Charles River LLC.). Specifically, each egg was infected with 50 PFU of IAV/PR8 in 100 μL of PBS/BSA/Penn-Strep as previously described (47) and incubated at 37 °C for 48 h. The eggs were then stored at 4 °C overnight, and the allantoic fluid was collected. The allantoic fluid was spun down at 4,000 rpm for 30 min at 4 °C. The supernatant was pooled, aliquoted, and stored at −80 °C. Virus titers were determined by plaque assay with MDCK cells.

Mouse Infection. Sex-matched suckling (6- to 8-d-old) or adult (6- to 8-wk-old) mice were used for immunization followed by challenge. Littermates were randomly assigned to experimental groups.

Immunization. Mice were infected by IP injection of live NoVΔB2 virus particle suspension. NoVΔB2 virus particle containing the same amount of virus was killed by UV exposure as control. Suckling mice were injected with 50 μL virus particle suspension titrated to contain 3×10^5 copies of the viral genomic RNA1 in the buffer as described previously (2, 10). Adult mice were injected with 150 μL virus particle suspension titrated to contain 4.5×10^9 copies of the viral genomic RNA1 in the buffer.

Challenge. For NoV challenge, mice were infected by ip injection of NoV virus particle suspension (50 μL containing 1.5×10^8 copies of the viral genomic RNA1 in the buffer for suckling mice and 150 μL containing 4.5×10^9 copies of the viral genomic RNA1 in the buffer for adult mice). For survival and body

weight change experiments, mock or virus-infected mice were observed for 4 to 6 wk postinfection. Virus inoculations were performed under anesthesia, and all efforts were made to minimize animal suffering. For challenge with CVB3, adult mice were ip injected with 100 μL CVB3 containing 1×10^8 PFU, while for IAV/PR8 challenge in adult mice, 50 μL of IAV/PR8 containing 50 PFU was given intranasally under isoflurane anesthesia.

RNA Extraction. Based on UCR IACUC guidelines, mice were euthanized with CO_2 followed by cervical dislocation, and the hind limb skeletal muscle tissues were collected in Eppendorf tubes with metal beads, flash-frozen in liquid nitrogen, and then stored at −80 °C. For RNA extraction, 1 mL of cold TRIzol Reagent was added to each tube and homogenized using TissueLyzer II (Qiagen). After removal of cell debris, total RNA was extracted by TRIzol Reagent.

Detection of the Viral RNA by Northern Blot Analysis. Northern blotting detection of the viral RNAs was conducted as described (2). Briefly, approximately 4 μg of total tissue RNA were analyzed using a ^{32}P α-dCTP (PerkinElmer) labeled DNA fragment corresponding to the B2 coding region of the NoV RNA1 and RNA3, for the detection of the viral genomic RNA1 and subgenomic RNA3.

Detection of the Viral RNA by RT-qPCR. As it was described previously (10), the RNA1 level of wild-type and mutant NoV in mouse tissue was quantitated with the RT-qPCR technique using β-actin mRNA as the internal reference. One μg of total tissue RNA was used for cDNA synthesis using iScript™ cDNA Synthesis Kit (Bio-Rad). The cDNA products were subjected to quantitative PCR with iQ SYBR green Supermix (Bio-Rad), using primers 5′-CCG TTC ATG GCT TAC ACC TT-3′ (NoV Fwd) and 5′-GCA CCA GTC CCA AAC TTC AT-3′ (NoV Rev); 5′-ATT GGC AAC GAG CGG TTC C-3′ (beta-actin Fwd) and 5′-AGC ACT GTG TTG GCA TAG AGG-3′ (beta-actin Rev).

Detection of the Viral Proteins by Western Blot Analysis. Western blot detection of NoV and mouse proteins was carried out as described previously (2). The hind limb skeletal muscle tissues were collected immediately after mice were killed and flash-frozen in liquid nitrogen in Eppendorf tubes prefilled with metal beads, and then stored at −80 °C until in use. After homogenization in 1× RIPA buffer (Cell Signaling) supplemented with cOmplete™ Protease Inhibitor Cocktail (Roche) and phosphatase inhibitor cocktail PhosStop™ (Roche) using TissueLyzer II (Qiagen), NoV B2 and CP proteins were probed with house-made polyclonal rabbit antibodies. Mouse glyceraldehyde 3-phosphate dehydrogenase (GAPDH) was probed with the mouse monoclonal anti-GAPDH antibody (Invitrogen, MA5-15738) and served as the sample loading control.

Antibiotics (Abx) Treatment. Adult mice were treated with Abx as described in literature (48) with some modification. Briefly, Abx cocktail (1 g/L ampicillin and 0.5 g/L vancomycin; from Sigma) in 20 g/L grape Kool-Aid (Kraft Foods) or Kool-Aid (vehicle) alone were added in drinking water throughout the whole length of the experiment.

Fecal pellets were collected pre- and 3 or 8 d post-Abx or vehicle treatment into screw-cap tube with 1 mm diameter zirconia/silica beads (Biospec). Fecal DNA was extracted with QIAamp Fast DNA Stool Mini Kit (QIAGEN) as instructed by the manufacturer. Bacterial 16S rDNA copies were detected by quantitative RT-PCR of the V4 hypervariable region of the 16S rRNA gene, with iQ SYBR green Supermix (Bio-Rad), using primers 515Fwd (5′-GTG CCA GCM GCC GCG GTA A-3′) and 805Rev (5′-GAC TAC CAG GGT ATC TAA TCC-3′).

Statistical Analysis. Mouse body weight changes were analyzed by multiple unpaired *t* test. Survival curves were compared by using a log rank (Mantel-Cox) test. Unpaired Student's *t* test was used for statistical analysis of RT-qPCR data. Body weight and RT-qPCR data are shown in mean ± SEM. All statistical analyses and graphs were performed using GraphPad Prism version 10.1.0.

Data, Materials, and Software Availability. All study data are included in the article and/or *SI Appendix*.

ACKNOWLEDGMENTS. We thank K.L. Johnson and L.A. Ball for cDNA clones of NoV and NoVΔB2, J.M. Bergelson for CVB3, and Ansel Hsiao for advice on microbiota depletion. This study was supported by NIH Grants AI52447, AI110579, and AI141887 as well as funding from the College of Natural and Agricultural Sciences, University of California, Riverside.

Author affiliations: [a]Department of Microbiology and Plant Pathology, University of California, Riverside, CA 92521

Author contributions: G.C., Q.H., W.-X.L., R.H., and S.-W.D. designed research; G.C., Q.H., W.-X.L., and R.H. performed research; G.C., Q.H., W.-X.L., R.H., and S.-W.D. analyzed data; and G.C., R.H., and S.-W.D. wrote the paper.

1. P. Parameswaran *et al.*, Six RNA viruses and forty-one hosts: Viral small RNAs and modulation of small RNA repertoires in vertebrate and invertebrate systems. *PLoS Pathog.* **6**, e1000764 (2010).
2. Y. Li, J. Lu, Y. Han, X. Fan, S. W. Ding, RNA interference functions as an antiviral immunity mechanism in mammals. *Science* **342**, 231–234 (2013).
3. P. V. Maillard *et al.*, Antiviral RNA interference in mammalian cells. *Science* **342**, 235–238 (2013).
4. Y. Li *et al.*, Induction and suppression of antiviral RNA interference by influenza A virus in mammalian cells. *Nat. Microbiol.* **2**, 16250 (2016).
5. Y. Qiu *et al.*, Human virus-derived small RNAs can confer antiviral immunity in mammals. *Immunity* **46**, 992–1004 (2017).
6. Y. P. Xu *et al.*, Zika virus infection induces RNAi-mediated antiviral immunity in human neural progenitors and brain organoids. *Cell Res.* **29**, 265–273 (2019).
7. Y. Qiu *et al.*, Flavivirus induces and antagonizes antiviral RNA interference in both mammals and mosquitoes. *Sci. Adv.* **6**, eaax7989 (2020).
8. F. Adiliaghdam *et al.*, A requirement for Argonaute 4 in mammalian antiviral defense. *Cell Rep.* **30**, 1690–1701.e1694 (2020).
9. Y. Zhang *et al.*, The activation of antiviral RNA interference not only exists in neural progenitor cells but also in somatic cells in mammals. *Emerging Microbes Infect.* **9**, 1580–1589 (2020).
10. Q. Han *et al.*, Mechanism and function of antiviral RNA interference in mice. *mBio* **11**, e03278-19 (2020).
11. Y. Fang *et al.*, Inhibition of viral suppressor of RNAi proteins by designer peptides protects from enteroviral infection in vivo. *Immunity* **54**, 2231–2244.e2236 (2021).
12. E. Z. Poirier *et al.*, An isoform of Dicer protects mammalian stem cells against multiple RNA viruses. *Science* **373**, 231–236 (2021).
13. Y. Zhang *et al.*, Efficient Dicer processing of virus-derived double-stranded RNAs and its modulation by RIG-I-like receptor LGP2. *PLoS Pathog.* **17**, e1009790 (2021).
14. Y. Zhang *et al.*, Mouse circulating extracellular vesicles contain virus-derived siRNAs active in antiviral immunity. *EMBO J.* **41**, e109902 (2022), 10.15252/embj.2021109902.
15. S. W. Ding, Q. Han, J. Wang, W. X. Li, Antiviral RNA interference in mammals. *Curr. Opin. Immunol.* **54**, 109–114 (2018).
16. Z. Guo, Y. Li, S. W. Ding, Small RNA-based antimicrobial immunity. *Nat. Rev. Immunol.* **19**, 31–44 (2019).
17. D. P. Anobile, E. Z. Poirier, RNA interference, an emerging component of antiviral immunity in mammals. *Biochem. Soc. Trans.* **51**, 137–146 (2023).
18. W. X. Li, S. W. Ding, Mammalian viral suppressors of RNA interference. *Trends Biochem. Sci.* **47**, 978–988 (2022).
19. S. W. Ding, RNA-based antiviral immunity. *Nat. Rev. Immunol.* **10**, 632–644 (2010).
20. S. Lopez-Gomollon, D. C. Baulcombe, Roles of RNA silencing in viral and non-viral plant immunity and in the crosstalk between disease resistance systems. *Nat. Rev. Mol. Cell Biol.* **23**, 645–662 (2022).
21. L. A. Ball, J. M. Amann, B. K. Garrett, Replication of nodamura virus after transfection of viral RNA into mammalian cells in culture. *J. Virol.* **66**, 2326–2334 (1992).
22. K. L. Johnson, B. D. Price, L. A. Ball, Recovery of infectivity from cDNA clones of nodamura virus and identification of small nonstructural proteins. *Virology* **305**, 436–451 (2003).
23. R. Aliyari *et al.*, Mechanism of induction and suppression of antiviral immunity directed by virus-derived small RNAs in Drosophila. *Cell Host Microbe* **4**, 387–397 (2008).
24. F. Krammer, P. Palese, Advances in the development of influenza virus vaccines. *Nat. Rev. Drug Discov.* **14**, 167–182 (2015).
25. P. Mombaerts *et al.*, RAG-1-deficient mice have no mature B and T lymphocytes. *Cell* **68**, 869–877 (1992).
26. P. Zimmermann, N. Curtis, The influence of the intestinal microbiome on vaccine responses. *Vaccine* **36**, 4433–4439 (2018).
27. D. J. Lynn, S. C. Benson, M. A. Lynn, B. Pulendran, Modulation of immune responses to vaccination by the microbiota: Implications and potential mechanisms. *Nat. Rev. Immunol.* **22**, 33–46 (2022).
28. Y. Shinkai *et al.*, RAG-2-deficient mice lack mature lymphocytes owing to inability to initiate V(D)J rearrangement. *Cell* **68**, 855–867 (1992).
29. J. Song *et al.*, A mouse model for the human pathogen *Salmonella typhi*. *Cell Host Microbe* **8**, 369–376 (2010).
30. J. P. Jayasekera, E. A. Moseman, M. C. Carroll, Natural antibody and complement mediate neutralization of influenza virus in the absence of prior immunity. *J. Virol.* **81**, 3487–3494 (2007).
31. H. Wu, V. Haist, W. Baumgartner, K. Schughart, Sustained viral load and late death in Rag2−/− mice after influenza A virus infection. *Virol. J.* **7**, 172 (2010).
32. P. Liu *et al.*, The tyrosine kinase p56lck is essential in coxsackievirus B3-mediated heart disease. *Nat. Med.* **6**, 429–434 (2000).
33. A. G. van der Veen *et al.*, The RIG-I-like receptor LGP2 inhibits Dicer-dependent processing of long double-stranded RNA and blocks RNA interference in mammalian cells. *EMBO J.* **37**, e97479 (2018), 10.15252/embj.201797479.
34. J. Wang, Y. Li, Current advances in antiviral RNA interference in mammals. *FEBS J.* **291**, 208–216 (2024).
35. B. S. Graham, J. R. Mascola, A. S. Fauci, Novel vaccine technologies: Essential components of an adequate response to emerging viral diseases. *JAMA* **319**, 1431–1432 (2018).
36. F. P. Polack *et al.*, Safety and efficacy of the BNT162b2 mRNA Covid-19 vaccine. *N. Engl. J. Med.* **383**, 2603–2615 (2020).
37. L. R. Baden *et al.*, Efficacy and safety of the mRNA-1273 SARS-CoV-2 vaccine. *N. Engl. J. Med.* **384**, 403–416 (2020).

38. H. A. Gans *et al.*, Deficiency of the humoral immune response to measles vaccine in infants immunized at age 6 months. *JAMA* **280**, 527–532 (1998).
39. M. Vazquez *et al.*, Effectiveness over time of Varicella vaccine. *JAMA* **291**, 851–855 (2004).
40. W. X. Li *et al.*, Interferon antagonist proteins of influenza and vaccinia viruses are suppressors of RNA silencing. *Proc. Natl. Acad. Sci. U.S.A.* **101**, 1350–1355 (2004).
41. J. Talon *et al.*, Influenza A and B viruses expressing altered NS1 proteins: A vaccine approach. *Proc. Natl. Acad. Sci. U.S.A.* **97**, 4309–4314 (2000).
42. R. Hai *et al.*, Influenza B virus NS1-truncated mutants: Live-attenuated vaccine approach. *J. Virol.* **82**, 10580–10590 (2008).
43. Y. Du *et al.*, Genome-wide identification of interferon-sensitive mutations enables influenza vaccine design. *Science* **359**, 290–296 (2018).
44. Q. Wu *et al.*, Virus discovery by deep sequencing and assembly of virus-derived small silencing RNAs. *Proc. Natl. Acad. Sci. U.S.A.* **107**, 1606–1611 (2010).
45. M. K. Slifka, R. Pagarigan, I. Mena, R. Feuer, J. L. Whitton, Using recombinant coxsackievirus B3 to evaluate the induction and protective efficacy of CD8+ T cells during picornavirus infection *J. Virol.* **75**, 2377–2387 (2001).
46. D. S. Kim, Y. L. Cho, B. G. Kim, S. H. Lee, J. H. Nam, Systematic analysis of attenuated expressing a foreign gene as a viral vaccine vector. *Vaccine* **28**, 1234–1240 (2010).
47. R. Hai *et al.*, Influenza A(H7N9) virus gains neuraminidase inhibitor resistance without loss of in vivo virulence or transmissibility. *Nat. Commun.* **4**, 2854 (2013).
48. E. S. Winkler *et al.*, The intestinal microbiome restricts alphavirus infection and dissemination through a bile acid-Type I IFN signaling axis. *Cell* **182**, 901–918.e918 (2020).